Phyton-
International Journal of
Experimental Botany

Tech Science Press

DOI: 10.32604/phyton.2023.045802

ARTICLE

Silicon Mitigates Aluminum Toxicity of Tartary Buckwheat by Regulating Antioxidant Systems

Anyin Qi[1,#], Xiaonan Yan[1,#], Yuqing Liu[1,#], Qingchen Zeng[1], Hang Yuan[1], Huange Huang[1], Chenggang Liang[2], Dabing Xiang[1], Liang Zou[1], Lianxin Peng[1], Gang Zhao[1], Jingwei Huang[1,*] and Yan Wan[1,*]

[1]Key Laboratory of Coarse Cereal Processing, Ministry of Agriculture and Rural Affairs, Sichuan Engineering & Technology Research Center of Coarse Cereal Industrialization, College of Food and Biological Engineering, Chengdu University, Chengdu, 610106, China

[2]Research Center of Buckwheat Industry Technology, School of Life Sciences, Guizhou Normal University, Guiyang, 550001, China

[*]Corresponding Authors: Jingwei Huang. Email: huangjingwei1003@sina.com; Yan Wan. Email: yanwan@cdu.edu.cn

[#]These authors equally contribute to this work

Received: 08 September 2023 Accepted: 14 November 2023 Published: 26 January 2024

ABSTRACT

Aluminum (Al) toxicity is a considerable factor limiting crop yield and biomass in acidic soil. Tartary buckwheat growing in acidic soil may suffer from Al poisoning. Here, we investigated the influence of Al stress on the growth of tartary buckwheat seedling roots, and the alleviation of Al stress by silicon (Si), as has been demonstrated in many crops. Under Al stress, root growth (total root length, primary root length, root tips, root surface area, and root volume) was significantly inhibited, and Al and malondialdehyde (MDA) accumulated in the root tips. At the same time, catalase (CAT) and ascorbate peroxidase activities, polyphenols, flavonoids, and 1,1-diphenyl-2-picryl-hydrazyl (DPPH) and 2,2′-azinobis-(3-ethylbenzthiazoline-6-sulphonate) (ABTS) free-radical scavenging ability were significantly decreased. After the application of Si, root growth, Al accumulation, and oxidative damage were improved. Compared to Al-treated seedlings, the contents of $\cdot O_2^-$ and MDA decreased by 29.39% and 25.22%, respectively. This was associated with Si-induced increases in peroxidase and CAT enzyme activity, flavonoid compounds, and free-radical scavenging (DPPH and ABTS). The application of Si therefore has positive effects on Al toxicity in tartary buckwheat roots by reducing Al accumulation in the roots and maintaining oxidation homeostasis.

KEYWORDS

Tartary buckwheat; aluminum stress; silicon; root growth; oxidative stress

1 Introduction

Aluminum (Al) accounts for about 7% of the Earth's crust [1]. When the soil pH is below 4.5, Al ions (Al^{3+}) appear and are toxic to plants [2]. Acid soils occupy 30% of the global land area and 40% of the world's arable soils, making Al toxicity an obstacle to crop growth and productivity [3]. Under acidic conditions, Al^{3+} is absorbed by the plants and disrupts a variety of metabolic processes, including destruction of the root cell wall structure, induction of oxidative stress, disruption of the plasma

membrane and signal-transduction pathways, and inhibition of polar auxin transport [4]. Inhibition of root elongation is the primary symptom of Al toxicity [5], resulting in restricted absorption of nutrients and water [6]. The photosynthetic system is also damaged via Al absorption and transfer to the aboveground plant parts [7,8]. Ultimately, Al toxicity results in reduced crop biomass and grain yield, and economic losses [9].

Silicon (Si) has been recognized as a beneficial mineral nutrient and the amount absorbed by plants is similar to that of macronutrients [10,11]. Si is usually present in the soil in the form of silicon dioxide, which plants cannot absorb [12]. Only silicic acid or silicate can be absorbed by plant root cells and then transferred to the aboveground parts through the xylem [13]. All plant tissues can accumulate Si [14], improving plants' nutrient uptake, photosynthetic capacity, and antioxidant potential, as well as biotic and abiotic stress resistance [15,16]. Si deposition on the root cell wall affects the entry of metal ions, including Al^{3+} [17], by reducing Al-binding sites on the cell wall polysaccharides [18,19]. The deposited Si also forms a complex with Al, and Si–Al compounds in the shoot have been found to aid in the internal detoxification of the plant [20]. Furthermore, Si can reduce the production of reactive oxygen species (ROS) caused by metal stress through improved antioxidant capacity [21]. In ryegrass, Si application alleviated lipid peroxidation triggered by Al stress by increasing phenol concentration and the activities of antioxidant enzymes such as superoxide dismutase (SOD), peroxidase (POD), catalase (CAT), and ascorbate peroxidase (APX) [22]. Similarly, Si mitigated abiotic stress by activating enzymes and the non-enzymatic antioxidant system (ascorbic acid and glutathione) in rice [23] and barley [24].

Tartary buckwheat is an important edible and medicinal crop with abundant nutrients and bioactive compounds [25]. The main production area of Tartary buckwheat is southwest China, where acidic red soils, yellow soils, and latosols with mostly low pH predominate [26,27]. Tartary buckwheat is an Al-accumulating species; plants subjected to 50 μM Al accumulated approximately 5 and 0.4 g kg^{-1} in the roots and shoots, respectively [28], and showed inhibited root growth [29]. One study found that Si enhances tartary buckwheat growth characteristics and fortifies the bioactive compounds [30]. Furthermore, there is evidence of Si alleviating Al toxicity in rice, maize, and peanut [31–33]. Therefore, the objective of this study was to investigate the effects of Si on root growth, ROS production, and the antioxidant system of Tartary buckwheat roots under Al stress.

2 Methods

2.1 Plant Material and Growth Conditions

Uniform-sized seeds of Tartary buckwheat (Chuanqiao No. 1) were sterilized in sodium hypochlorite solution for 15 min, then washed thoroughly with ultrapure water and soaked in ultrapure water for 12 h. The soaked seeds were placed on a seedling tray with a layer of gauze and germinated at 18°C/25°C and 70%/80% humidity (day/night) in the dark for 3 days. Extra ultrapure water was added regularly during germination to keep the gauze moist. Uniform germinated seeds with 2 cm root length were selected and placed in a PCR plate with no bottom. Each PCR plate containing 30 germinated seeds was floated in a square box containing 400 ml of different treatment solutions, and growth was continued at 18°C/25°C, 70%/80% humidity, in a 12/12 h (light/dark) environment for 4 days. Seedlings were harvested and assayed.

2.1.1 Al Stress Experiment

This experiment was carried out using hydroponics. Different concentrations of aluminum trichloride ($AlCl_3$) were added to a base nutrient solution of 0.5 mM calcium chloride ($CaCl_2$), and the pH was adjusted to 4.5 with potassium hydroxide (KOH) and hydrochloric acid (HCl). The treatment groups were: CK (control, only base nutrient solution), and CK (pH 4.5) with 25, 50, 100, 200, or 300 μM Al^{3+} (from $AlCl_3$).

2.1.2 Si Mitigation of Al Stress Experiment

This experiment was also carried out using hydroponics. We applied 1.5 mM sodium silicate (Na_2SiO_3) based on preliminary experimental results (shown in the supplementary materials), and 100 μM Al^{3+}, based on the results in Table 1 and its actual amount in acidic soil [34], to study the influence of Si on Al stress. Treatments were: base nutrient solution (CK), and addition of 1.5 mM Na_2SiO_3 (CK+Si), 100 μM Al^{3+} (Al), or 1.5 mM Na_2SiO_3 + 100 μM Al^{3+} (Al+Si). The pH of all solutions was maintained at 4.5 by KOH and HCl. The seeds were cultivated under the same conditions as in Section 2.1.1. After 4 days, some of the seedlings were used to determine morphological parameters, and the rest were frozen in liquid nitrogen and stored at −80°C.

Table 1: Root and shoot growth of Tartary buckwheat seedlings treated with (A) different concentrations of Al^{3+} (means ± SE, n = 15) and (B) the addition of Si under 100 μM Al^{3+} stress (means ± SE, n = 30)

	Treatment	Total root length (cm)	Main root length (cm)	Root tips (number)	Root surface area (cm^2)	Root volume (cm^3)	Shoot length (cm)
A	CK	46.29 ± 2.08a	13.47 ± 0.67a	105.93 ± 10.69b	9.19 ± 0.49a	0.0208 ± 0.001a	8.35 ± 0.25a
	CK(pH 4.5)	42.12 ± 1.71b	10.07 ± 0.94b	131.87 ± 14.09a	8.78 ± 0.48a	0.0224 ± 0.0011a	6.19 ± 0.2cd
	25 μM Al^{3+}	39.69 ± 1.03b	8.38 ± 0.67b	98.87 ± 6.28bc	8.36 ± 0.32a	0.0198 ± 0.0011ab	6.44 ± 0.17cd
	50 μM Al^{3+}	33.26 ± 1.05c	6.47 ± 0.59c	81.53 ± 5.49cd	6.84 ± 0.28b	0.0172 ± 0.0006bc	5.9 ± 0.19d
	100 μM Al^{3+}	22.05 ± 1.17d	5.42 ± 0.4c	63.13 ± 7.38de	5.32 ± 0.24c	0.0157 ± 0.001c	6 ± 0.38d
	200 μM Al^{3+}	15.58 ± 0.59e	3.06 ± 0.44d	51.93 ± 3.58e	5.07 ± 0.2c	0.0127 ± 0.001d	6.85 ± 0.29bc
	300 μM Al^{3+}	14.4 ± 0.79e	2.29 ± 0.23d	45.67 ± 3.02e	4.59 ± 0.22c	0.0126 ± 0.0008d	7.36 ± 0.25b
B	CK	29.51 ± 1.31a	7.65 ± 0.28ab	92.57 ± 6ab	6.1 ± 0.23a	0.0196 ± 0.0006a	8.43 ± 0.27ab
	CK+Si	28.97 ± 1.17a	8.43 ± 0.43a	105.37 ± 6.91a	6.16 ± 0.26a	0.0174 ± 0.0006b	8.32 ± 0.18b
	Al	21.97 ± 0.81b	5.89 ± 0.19c	60.47 ± 5.04c	5.15 ± 0.19b	0.017 ± 0.0007b	8.07 ± 0.27b
	Al+Si	23.25 ± 0.82b	7.19 ± 0.41b	87.13 ± 4.53b	5.8 ± 0.23a	0.0184 ± 0.0009ab	9.12 ± 0.27a

Note: CK = 0.5 mM $CaCl_2$, CK+Si = 0.5 mM $CaCl_2$ + 1.5 mM Na_2SiO_3, Al = 0.5 mM $CaCl_2$ + 100 μM Al^{3+}, Al+Si = 0.5 mM $CaCl_2$ + 100 μM Al^{3+} + 1.5 mM Na_2SiO_3. Different letters in the same column indicate statistically significant differences according to Duncan's test ($p < 0.05$).

2.2 Growth Analysis

For each treatment, 15 Tartary buckwheat seedlings were randomly selected (Excel's RANDBETWEEN function) for morphological parameter determination. Lengths of the primary root and shoot were measured with a ruler. All roots were imaged by a root scanner (Epson Expression 12000xl scanner, Japan) to determine total root length, root tips, root volume, and root surface area using 2017WinRHIZO software.

2.3 Superoxide Anions and Malondialdehyde

Superoxide anions (O_2^-) were measured using the Superoxide Anion Activity Content Assay Kit (Solarbio Life Sciences, BC1295, China). The content of malondialdehyde (MDA) was determined by the

thiobarbituric acid method as conducted by Nahar et al. [35]. A 0.1 g sample was extracted by homogenization in 1 ml 10 trichloroacetic acid and centrifugation. Then 0.5 ml supernatant was added to the same volume of thiobarbituric acid solution. The solution was placed in a boiling water bath for 15 min, cooled, and centrifuged, and MDA content was determined by spectrophotometry (UNICOSH, UV-2600A, China).

2.4 Antioxidant Enzyme Activity

A 0.1 g sample of roots was mixed with 1 ml of 0.05 M sodium phosphate buffer (pH 7.8) with 1% (w/v) polyvinylpyrrolidone, and then ground into homogenate in a freezing grinder. The mixture was centrifuged at 4°C and 12,000 rpm for 20 min, and the supernatant was collected for the measurement of antioxidant enzyme activities [35] as follows.

SOD enzyme activity was determined by preparing a reaction solution consisting of 1.5 ml of 50 mM sodium phosphate buffer (pH 7.8), 0.3 ml of 0.75 mM NBT, 100 µM EDTA, 130 mM L-methionine, 20 µM riboflavin, 0.5 ml of distilled water and 50 µl enzyme extract. The test tube was exposed to light for 30 min and then moved to a dark environment to stop the reaction and determine activity [36].

POD enzyme activity was determined according to MacAdam et al. [37]. The reaction solution was prepared with 50 ml of 50 mM sodium phosphate buffer (pH 6.0), adding 28 µl methoxyphenol and heating until dissolved, cooling, and adding 19 µl hydrogen peroxide (H_2O_2). A 0.1 ml aliquot of enzyme solution was added into 3 ml of reaction solution and after 30 s, the change in absorbance at 470 nm was monitored for 1 min.

CAT activity was determined as in Chance et al. [38]. The reaction solution was prepared by mixing 20 ml phosphate buffer (0.1 M, pH 7.0) with 80 ml H_2O_2 (0.1 mM). A 2.5 ml aliquot of reaction solution was added to 0.1 ml enzyme solution, and 30 s later, the change in absorbance at 240 nm was monitored for 1 min.

APX activity was determined according to Nakano et al. [39]: 0.1 ml enzyme solution was added to 2.70 ml phosphate buffer (0.05 M, pH 7.0, containing 0.1 mM EDTA-Na), 0.1 ml of 15 mM ascorbic acid, and 0.1 ml of 30 mM hydrogen peroxide. The change in absorbance at 240 nm was monitored for 1 min.

2.5 Total Polyphenol, Total Flavonoid, and Free Radical-Scavenging Ability

Roots (1 g FW) were homogenized with 5 ml 80% methanol, then broken ultrasonically at 50°C for 30 min and centrifuged at 10,000 rpm for 15 min. The supernatant was separated for analysis of total polyphenol and total flavonoid contents, and free radical-scavenging ability. Total polyphenols and total flavonoids were quantified using the method described by Wan et al. [40]. To determine the total polyphenol: 0.5 ml of the extracted solution was mixed with 2.5 ml of 0.2 M Folin–Ciocalteu reagent and reacted for 5 min. Then 2 ml of 7.5% sodium carbonate was added and the mixture was kept in the dark for 2 h. The absorbance of the solution was measured at 760 nm. To determine the total flavonoid: 1.0 ml extraction solution was added to 0.5 ml of 5% sodium nitrite and 0.5 ml of 10% $AlCl_3$ and reacted for 5 min. Then 2.5 mL of 1 M sodium hydroxide was added to terminate the reaction. The absorbance of the solution was measured at 500 nm.

Free radical-scavenging ability (1,1-diphenyl-2-picrylhydrazyl (DPPH)) and 2,2′-azinobis-(3-ethylbenzthiazoline-6-sulphonate (ABTS)) was estimated using the method of Sarker and Oba [41]. Antioxidant activity was determined by DPPH as follows: 50 µl of extract solution was added to a tube containing 950 µl of distilled water and 2 ml of 0.1 mM DPPH. The absorbance of the solution was measured at 517 nm after the tube was left at room temperature for 30 min. Antioxidant activity was determined by ABTS as follows: a stock solution was prepared with 7 mM ABTS solution and 7.35 mM

potassium persulfate solution, which were mixed and left standing for 12 h at room temperature in the dark. Then 50 µl extraction solution, 950 µl distilled water, and 2.0 ml ABTS (1 ml of stock solution mixed with 60 ml of 80% methanol) were mixed and allowed to react in the dark for 2 h. The absorbance of the solution was measured at 734 nm.

2.6 Hematoxylin Staining of Roots

The presence of Al was indicated using hematoxylin as described by Kong et al. [42]. The roots were rinsed and soaked in distilled water three times for 10 min each time. Root tips were transferred to 0.2% (w/v) hematoxylin and 0.02% (w/v) potassium iodide for 30 min in the dark. Root tips were then completely dispersed in distilled water, and observed and photographed under a stereomicroscope (Olympus, SZX16).

2.7 Statistical Analysis

Seedling morphology was analyzed by 15 or 30 strains respectively. Physiological data were statistically analyzed three times. Statistical data were analyzed using ANOVA in IBM SPSS Statistics 25, and Duncan's test was used to analyze significant differences. The images were created using Origin 2023 and Adobe Illustrator CC 2018 software.

3 Results

3.1 Seedling Growth Responses under Al Toxicity

The germinated tartary buckwheat seedlings were cultivated under acidic conditions with different concentrations of Al^{3+} for 4 days. The results are shown in Table 1A and Fig. 1A. Primary root length, total root length, and shoot length were significantly decreased under acidic conditions (pH 4.5) compared to seedlings grown under control conditions (0.5 mM $CaCl_2$). Root growth (total root length, primary root length, root tips, root surface area, and root volume) decreased significantly with increasing concentrations of Al^{3+}. Shoot length first decreased and then increased with increasing Al^{3+} concentration.

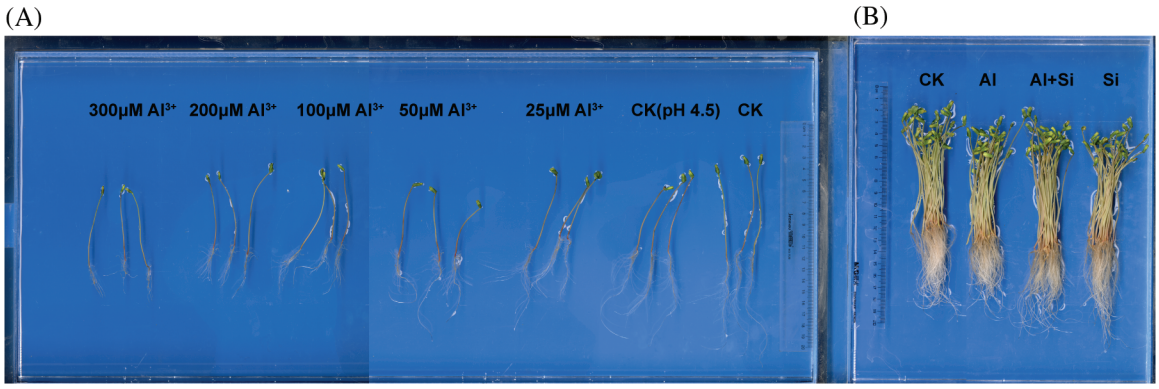

Figure 1: Root and shoot growth of Tartary buckwheat seedlings treated with different Al^{3+} concentrations (A) and with Si under 100 µM Al stress (B)

3.2 Effect of Si on Seedling Growth Responses under Al Toxicity

In the presence of Si, root growth (primary root length, root tips, and root surface area) and shoot length were significantly improved in comparison to the Al treatment (Table 1B and Fig. 1B), increasing by 22.06%, 44.10%, 12.55%, and 12.96%, respectively.

3.3 Hematoxylin Staining of Roots

Hematoxylin staining revealed the accumulation of Al in root tips under different treatments (Fig. 2). Under the Al treatments, intense staining in the root tips (including the root crown, meristem, and elongation regions) and older root zones was observed. In comparison, under the Al+Si treatment, the Al staining of the root tips was lighter, and the older root area had barely any stain at all.

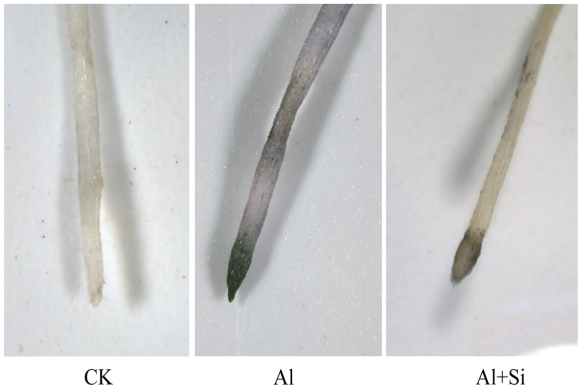

Figure 2: Hematoxylin staining of Tartary buckwheat roots under control (CK), 100 μM Al^{3+} (Al), and 100 μM Al^{3+} + 1.5 mM Na_2SiO_3 (Al+Si) treatments

3.4 Effect of Si on Biochemical Traits of Seedling Root Responses under Al Toxicity

3.4.1 $\cdot O_2^-$ and MDA

As shown in Fig. 3, the contents of $\cdot O_2^-$ and MDA in the roots of tartary buckwheat seedlings increased upon Al stress. The addition of Si significantly reduced these contents by 29.39% and 25.22%, respectively.

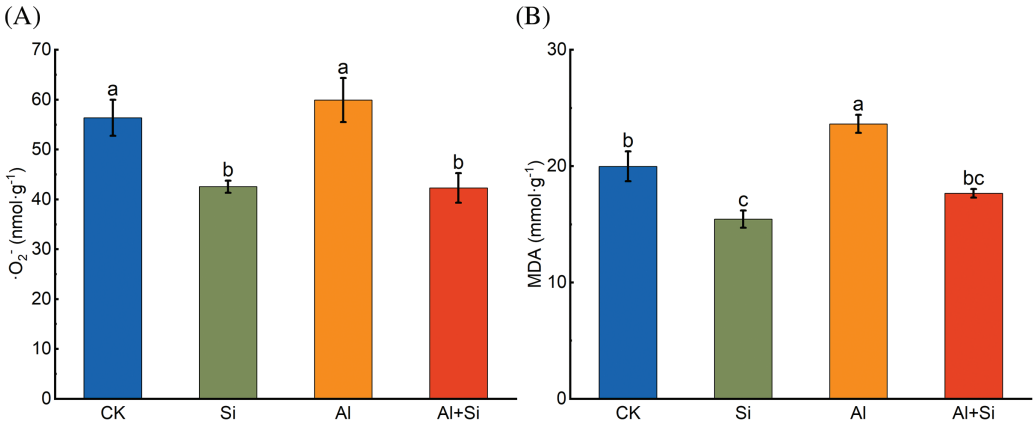

Figure 3: O_2^- (A) and MDA (B) content in the roots of tartary buckwheat seedlings under control (CK), 1.5 mM Na_2SiO_3 (Si), 100 μM Al^{3+} (Al), and 100 μM Al^{3+} + 1.5 mM Na_2SiO_3 (Al+Si) treatments. Values are means ± SE (n = 3) and different letters indicate statistically significant differences according to Duncan's test ($p < 0.05$)

3.4.2 Antioxidant Enzyme Activity

Under Al stress, SOD and POD activities were significantly enhanced compared to controls, whereas CAT and APX activities showed the opposite trend (Fig. 4). Exogenous application of Si resulted in a

further significant increase in POD activity and considerably alleviated the APX activity decline induced by the Al stress.

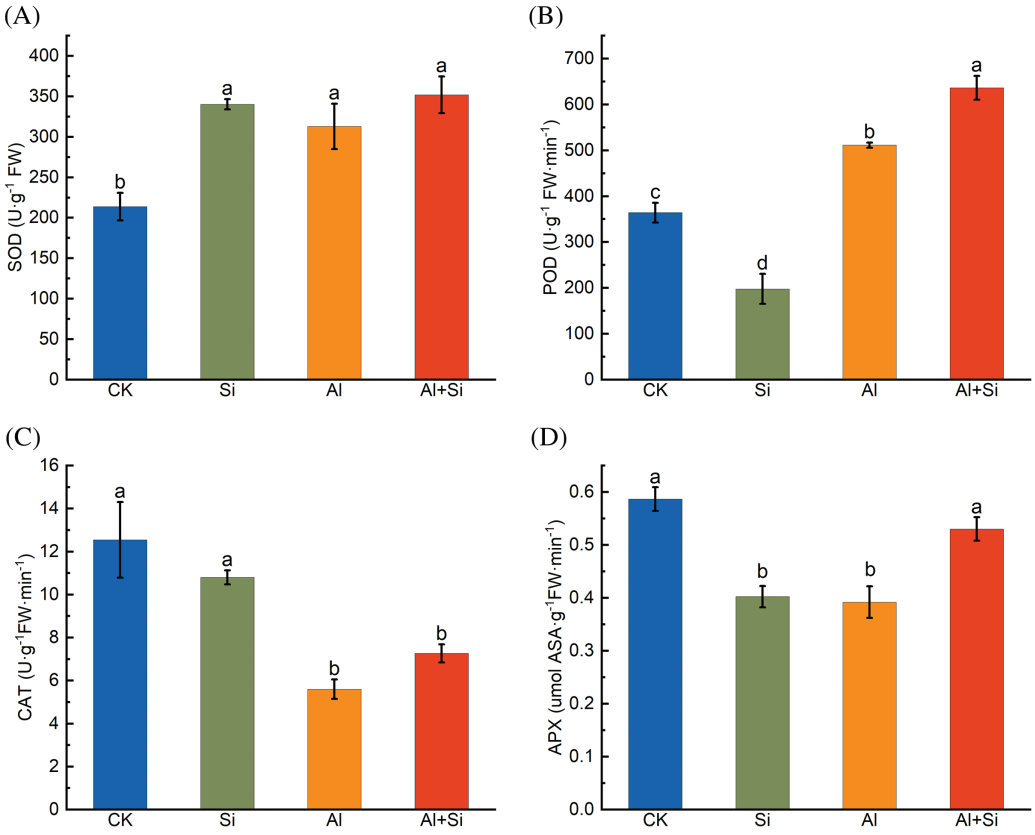

Figure 4: SOD (A), POD (B), CAT (C), and APX (D) activities in the roots of Tartary buckwheat seedlings under control (CK), 1.5 mM Na_2SiO_3 (Si), 100 μM Al^{3+} (Al), and 100 μM Al^{3+}+ 1.5 mM Na_2SiO_3 (Al+Si) treatments. Values are means ± SE (n = 3) and different letters indicate statistically significant differences according to Duncan's test ($p < 0.05$)

3.4.3 Polyphenol and Flavonoid Contents, and Free Radical-Scavenging Ability

Total polyphenol and total flavonoid contents, and free radical-scavenging ability by DPPH and ABTS assay were significantly reduced by Al stress (Fig. 5). These parameters were improved by adding Si, increasing by 18.42%, 37.78%, 47.28%, and 19.44% relative to the Al stress conditions, respectively.

3.5 Evaluation of the Effect of Si on Al Stress Using Hierarchical Clustering Heat Maps

Hierarchical clustering heat maps (Fig. 6) showed that root growth (total root length, primary root length, root tips, root surface area, and root volume), shoot length, polyphenol and flavonoid contents, free radical-scavenging ability (DPPH and ABTS), and APX activity were lower under the Al stress compared to controls, while $\cdot O_2^-$, MDA and soluble protein contents, and SOD and POD activities were higher. Compared to the Al treatment, the application of Si effectively increased root growth, shoot length, polyphenol, and flavonoid levels, free radical-scavenging ability, antioxidant enzyme activity (SOD, POD, CAT, and APX), and soluble protein content, and decreased $\cdot O_2^-$ and MDA contents.

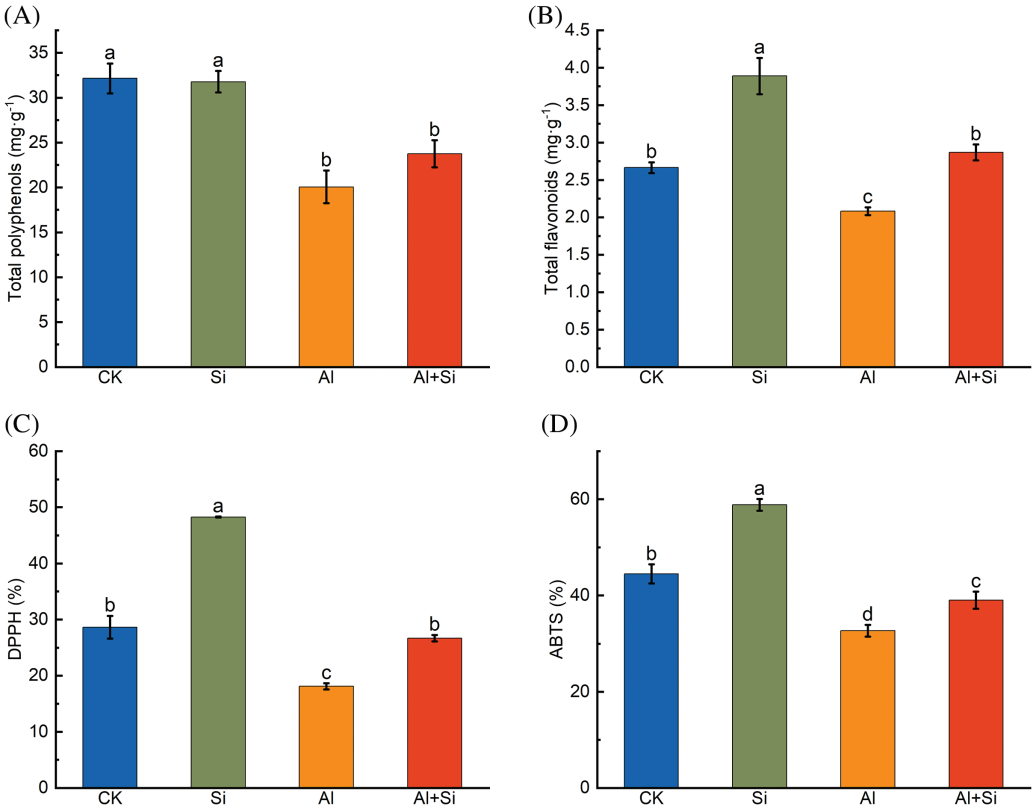

Figure 5: Total polyphenols (A), total flavonoids (B), and DPPH (C) and ABTS (D) free radical clearance in the roots of Tartary buckwheat seedlings under control (CK), 1.5 mM Na_2SiO_3 (Si), 100 μM Al^{3+} (Al), and 100 μM Al^{3+} + 1.5 mM Na_2SiO_3 (Al+Si) treatments. Values are means ± SE (n = 3) and different letters indicate statistically significant differences according to Duncan's test ($p < 0.05$)

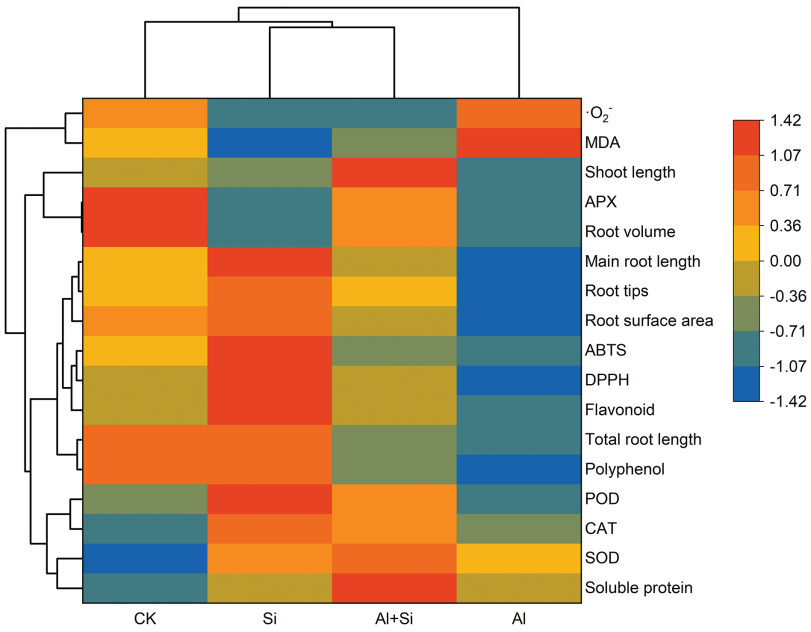

Figure 6: Hierarchical clustering heat maps of the Tartary buckwheat seedlings under control (CK), 1.5 mM Na_2SiO_3 (Si), 100 μM Al^{3+} (Al), and 100 μM Al^{3+} + 1.5 mM Na_2SiO_3 (Al+Si) treatments

4 Discussion

Root growth inhibition is one of the main and most severe indications of Al toxicity [43]. Upon exposure to Al^{3+}, Al binds quickly to the root tip cell walls, inhibiting their growth [44]. Significant inhibition of root growth by Al exposure is time- and concentration-dependent [45]. In the present study, when exposed to different Al concentrations for 4 days, root growth inhibition (total root length, primary root length, root tips, root surface area, and root volume) of Tartary buckwheat seedlings increased with increasing Al concentration (Table 1A). Consistent with our study, inhibition of these root characteristics was recorded in 227 common bean genotypes under Al toxicity [46]. However, the addition of Si significantly improved root growth under Al stress (Table 1B, Fig. 1B). This effect of Si has been verified in cucumber [47] and maize [48], and is associated with reduced deposition of Al in the root tips, as found in rice [49]. Similarly, hematoxylin staining for Al in the root tip was significantly weakened in the presence of Si + Al (Fig. 2). Previous studies have shown that Si can induce root exudation and regulate hemicellulose to affect the absorption and diffusion of Al [49,50].

Redox homeostasis plays an important role in root development, where excessive accumulation of ROS under Al stress can damage root cell development by causing protein oxidation, lipid peroxidation, and DNA damage [51,52]. The production of ROS, such as superoxide radicals ($\cdot O_2^-$), H_2O_2, and hydroxyl radicals (·OH), caused by Al toxicity has an important effect on plants [53]. In the present study, MDA content was significantly induced by Al (Fig. 3), reflecting disruption of plasma membrane integrity [54]. When Al is removed, ROS decreases and root elongation resumes [2]. Similarly, less O_2^- and MDA were accumulated in the roots of Al-tolerant soybean and wheat, respectively, exposed to Al [55,56]. The addition of Si significantly decreased $\cdot O_2^-$ and MDA content (Fig. 3). This means that Si enhances the plant's ability to tolerate Al, as also seen in barley [57] and wheat [58].

Under stress conditions, plants can regulate ROS homeostasis via their antioxidant enzymes [59]. Under Al stress, the activities of antioxidant enzymes SOD, POD, and CAT increase to cope with the increase in ROS, but when the tolerance range is exceeded, the antioxidant enzyme activities decrease and are insufficient to cope with the excess ROS, resulting in inhibition of plant root growth [60]. In one study, the addition of Si enhanced the activities of SOD, POD, CAT, and APX under Al stress, thereby reducing the contents of O_2^-, H_2O_2, and MDA, and reducing the toxicity of Al caused by peroxidation damage [23]. In the present study, Si supplementation significantly improved POD and APX activities, but did not improve SOD or CAT activities compared to the Al-treated seedlings (Fig. 4). The observed improvement in POD and APX activities may be an important factor in the alleviation of Al toxicity [61]. Under Al stress, SOD and POD activities were significantly increased, whereas CAT and APX activities were significantly decreased (Fig. 4). Decreased oxidase activity was also found in *Brassica napus*, possibly causing ROS accumulation [62]. Why Al stress reduces oxidase activities of CAT AND APX), and how the addition of Si improves activities of POD AND APX remains to be studied.

Phenolic compounds play multiple roles in plants' response to Al stress, such as protecting plants from oxidative stress, chelating Al to form Al–phenol complexes, and causing the efflux of Al^{3+} [63–65]. Previous studies have shown the induction of phenolic compounds upon Al stress [66]. In contrast, we found that Al toxicity damaged the synthesis of polyphenol and flavonoid compounds, and decreased free radical-scavenging capacity (DPPH and ABTS) in Tartary buckwheat seedling roots (Fig. 5). Si application significantly improved total flavonoids and free radical-scavenging capacity (Fig. 5), possibly serving to maintain ROS homeostasis [67]. Vega et al. [57] and Pontigo et al. [22] have shown that the enhancement of phenolic compounds triggered by Si contributes to relieving Al-induced oxidative stress in barley and ryegrass, respectively.

Overall, under Al stress, Al^{3+} accumulated in the roots of Tartary buckwheat seedlings, causing oxidative stress that disrupted root growth. The addition of Si alleviated the Al-induced oxidative damage

by enhancing antioxidant enzyme activities (POD and APX), phenolic (flavonoid) content, and free radical-scavenging capacity (DPPH and ABTS), and reducing the accumulation of Al^{3+} in the roots, thus improving root growth in tartary buckwheat seedlings (Fig. 6).

5 Conclusion

In this study, root growth of Tartary buckwheat seedlings was significantly inhibited by Al toxicity, which was related to the accumulation of large amounts of Al and oxidative damage. The application of Si reversed these adverse effects, mainly through a decrease in Al accumulation, and increased antioxidant enzyme activity and flavonoid compounds. Further study at the molecular and cellular levels will enhance our understanding of Si's alleviation of Al stress in Tartary buckwheat. The mitigating effect of Si application to Al-contaminated land on plants needs to be further verified.

Acknowledgement: We thank Camille Vainstein for her assistance in revising the paper.

Funding Statement: This work was supported by Science & Technology Department of Sichuan Province (2022YFQ0041, 2022NSFSC1725, 2023NSFSC0214); China Agriculture Research System (CARS-07-B-1); The National Natural Science Foundation of China (32160428); Innovative Training Program for College Students (202311079040, S202311079112, CDUCX2023550); Undergraduate Education and Teaching Reform Project of Chengdu University (cdjgb2022186).

Author Contributions: Study conception and design, Anyin Qi, Yan Wan, Jingwei Huang; data collection, Xiaonan Yan, Yuqing Liu, Qingchen Zeng; analysis and interpretation of results, Hang Yuan, Huangge Huang; writing—original draft preparation, Anyin Qi, Xiaonan Yan, Yuqing Liu; writing—review and editing, Jingwei Huang, Chenggang Liang, Dabing Xiang, Yan Wan; supervision, Liang Zou, Lianxin Peng, Gang Zhao; project administration, Dabing Xiang, Liang Zou, Lianxin Peng, Gang Zhao; funding acquisition, Yan Wan, Chenggang Liang, Dabing Xiang. All authors reviewed the results and approved the final version of the manuscript.

Availability of Data and Materials: The datasets used and/or analyzed during the current study are available from the author and/or corresponding author on reasonable request.

Ethics Approval: Not applicable.

Conflicts of Interest: The authors declare that they have no conflicts of interest to report regarding the present study.

References

1. Dai B, Chen C, Liu Y, Liu L, Qaseem MF, Wang J, et al. Physiological, biochemical, and transcriptomic responses of Neolamarckia cadamba to aluminum stress. Int J Mol Sci. 2020;21(24):9624.
2. Matsumoto H, Motoda H. Aluminum toxicity recovery processes in root apices. Possible association with oxidative stress. Plant Sci. 2012;185–186:1–8.
3. von Uexküll HR, Mutert E. Global extent, development and economic impact of acid soils. Plant Soil. 1995;171(1):1–15.
4. Ma JF. Syndrome of aluminum toxicity and diversity of aluminum resistance in higher plants. Int Rev Cytol. 2007;264(2007):225–52.
5. Ryan PR, Ditomaso JM, Kochian LV. Aluminium toxicity in roots: an Investigation of spatial sensitivity and the role of the root cap. J Exp Bot. 1993;44(259):437–46.
6. Liu H, Zhu R, Shu K, Lv W, Wang S, Wang C. Aluminum stress signaling, response, and adaptive mechanisms in plants. Plant Signal Behav. 2022;17(1):2057060.

7. Cheng X, Fang T, Zhao E, Zheng B, Huang B, An Y, et al. Protective roles of salicylic acid in maintaining integrity and functions of photosynthetic photosystems for alfalfa (*Medicago sativa* L.) tolerance to aluminum toxicity. Plant Physiol Biochem. 2020;155(2020):570–8.
8. Su L, Lv A, Wen W, Zhou P, An Y. Auxin is involved in magnesium-mediated photoprotection in photosystems of alfalfa seedlings under aluminum stress. Front Plant Sci. 2020;11(2020):746.
9. Purcell LC, Keisling TC, Sneller CH. Soybean yield and water extraction in response to deep tillage and high soil aluminum. Commun Soil Sci Plan. 2002;33(19–20):3723–35.
10. Bakhat HF, Bibi N, Zia Z, Abbas S, Hammad HM, Fahad S, et al. Silicon mitigates biotic stresses in crop plants: a review. Crop Prot. 2018;104:21–34.
11. Ma JF, Yamaji N. A cooperative system of silicon transport in plants. Trends Plant Sci. 2015;20(7):435–42.
12. Meena V, Dotaniya ML, Saha JK, Patra AK. Silicon potential to mitigate plant heavy metals stress for sustainable agriculture: a review. Silicon. 2022;14(9):4447–62.
13. Yadav M, George N, Dwibedi V. Emergence of toxic trace elements in plant environment: insights into potential of silica nanoparticles for mitigation of metal toxicity in plants. Environ Pollut. 2023;333:122112.
14. Cooke J, Leishman MR. Is plant ecology more siliceous than we realise? Trends Plant Sci. 2011;16(2):61–8.
15. Mandlik R, Thakral V, Raturi G, Shinde S, Nikolić M, Tripathi DK, et al. Significance of silicon uptake, transport, and deposition in plants. J Exp Bot. 2020;71(21):6703–18.
16. Kovács S, Kutasy E, Csajbók J. The multiple role of silicon nutrition in alleviating environmental stresses in sustainable crop production. Plants. 2022;11(9):1223.
17. Pavlovic J, Kostic L, Bosnic P, Kirkby EA, Nikolic M. Interactions of silicon with essential and beneficial elements in plants. Front Plant Sci. 2021;12:697592.
18. Wang Y, Stass A, Horst WJ. Apoplastic binding of aluminum is involved in silicon-induced amelioration of aluminum toxicity in maize. Plant Physiol. 2004;136(3):3762–70.
19. Jiang D, Wu H, Cai H, Chen G. Silicon confers aluminium tolerance in rice via cell wall modification in the root transition zone. Plant Cell Environ. 2022;45(6):1765–78.
20. Britez RM, Watanabe T, Jansen S, Reissmann CB, Osaki M. The relationship between aluminium and silicon accumulation in leaves of *Faramea marginata* (*Rubiaceae*). New Phytol. 2002;156(3):437–44.
21. Kim YH, Khan AL, Waqas M, Lee IJ. Silicon regulates antioxidant activities of crop plants under abiotic-induced oxidative stress: a review. Front Plant Sci. 2017;8(2017):510.
22. Pontigo S, Godoy K, Jiménez H, Gutiérrez-Moraga A, Mora MDLL, Cartes P, et al. Silicon-mediated alleviation of aluminum toxicity by modulation of Al/Si uptake and antioxidant performance in ryegrass plants. Front Plant Sci. 2017;8:642.
23. Jiang D, Xu H, Zhang Y, Chen G. Silicon mediated redox homeostasis in the root-apex transition zone of rice plays a key role in aluminum tolerance. Plant Physiol Biochem. 2023;201:107871.
24. Akhter MS, Noreen S, Ummara U, Aqeel M, Saleem N, Ahmed MM, et al. Silicon-induced mitigation of NaCl stress in barley (*Hordeum vulgare* L.), associated with enhanced enzymatic and non-enzymatic antioxidant activities. Plants. 2022;11(18):2379.
25. Zou L, Wu DT, Ren GX, Hu YC, Peng LX, Zhao J, et al. Bioactive compounds, health benefits, and industrial applications of Tartary buckwheat (*Fagopyrum tataricum*). Crit Rev Food Sci Nutr. 2021;63(5):1–17.
26. Xiang D, Song Y, Wu Q, Ma C, Zhao J, Wan Y, et al. Relationship between stem characteristics and lodging resistance of Tartary buckwheat (*Fagopyrum tataricum*). Plant Prod Sci. 2019;22(2):202–10.
27. Zhu Q, De Vries W, Liu X, Zeng M, Hao T, Du E, et al. The contribution of atmospheric deposition and forest harvesting to forest soil acidification in China since 1980. Atmospheric Environ. 2016;146:215–22.
28. Wang H, Chen RF, Iwashita T, Shen RF, Ma JF. Physiological characterization of aluminum tolerance and accumulation in tartary and wild buckwheat. New Phytol. 2015;205(1):273–9.
29. Zhu H, Wang H, Zhu Y, Zou J, Zhao FJ, Huang CF, et al. Genome-wide transcriptomic and phylogenetic analyses reveal distinct aluminum-tolerance mechanisms in the aluminum-accumulating species buckwheat (*Fagopyrum tataricum*). BMC Plant Biol. 2015;15(1):16.

30. Azad MOK, Park BS, Adnan M, Germ M, Kreft I, Woo SH, et al. Silicon biostimulant enhances the growth characteristics and fortifies the bioactive compounds in common and Tartary buckwheat plant. J Crop Sci Biotechnol. 2020;24(1):51–9.
31. Xiao Z, Ye M, Gao Z, Jiang Y, Zhang X, Nikolic N, et al. Silicon reduces aluminum-induced suberization by inhibiting the uptake and transport of aluminum in rice roots and consequently promotes root growth. Plant Cell Physiol. 2022;63(3):340–52.
32. Delavar K, Ghanati F, Zare-Maivan H, Behmanesh M. Effects of silicon on the growth of maize seedlings under normal, aluminum, and salinity stress conditions. J Plant Nutr. 2017;40(10):1475–84.
33. Dong Z, Li Y, Xiao X, Chen Y, Shen X. Silicon effect on growth, nutrient uptake, and yield of peanut (*Arachis hypogaea* L.) under aluminum stress. J Plant Nutr. 2018;41(15):2001–8.
34. Rutkowska B, Szulc W, Hoch M, Spychaj-Fabisiak E. Forms of Al in soil and soil solution in a long-term fertilizer application experiment. Soil Use Manage. 2015;31(1):114–20.
35. Nahar K, Hasanuzzaman M, Alam MM, Fujita M. Roles of exogenous glutathione in antioxidant defense system and methylglyoxal detoxification during salt stress in mung bean. Biol Plantarum. 2015;59(4):745–56.
36. Giannopolitis CN, Ries SK. Superoxide dismutases: I. Occurrence in higher plants. Plant Physiol. 1977;59(2): 309–14.
37. MacAdam JW, Nelson CJ, Sharp RE. Peroxidase activity in the leaf elongation zone of tall fescue: I. Spatial distribution of ionically bound peroxidase activity in genotypes differing in length of the elongation zone. Plant Physiol. 1992;99(3):872–8.
38. Chance B, Maehly AC. Assay of catalases and peroxidases. Method Enzym. 1955;2(1955):764–75.
39. Nakano Y, Asada K. Hydrogen peroxide is scavenged by ascorbate-specific peroxidase in spinach chloroplasts. Plant Cell Physiol. 1981;22(5):867–80.
40. Wan Y, Zhou M, Le L, Gong X, Jiang L, Huang J, et al. Evaluation of morphology, nutrients, phytochemistry and pigments suggests the optimum harvest date for high-quality quinoa leafy vegetable. Sci Horticul. 2022;304:111240.
41. Sarker U, Oba S. Drought stress enhances nutritional and bioactive compounds, phenolic acids and antioxidant capacity of Amaranthus leafy vegetable. BMC Plant Biol. 2018;18(1):258.
42. Kong X, Peng Z, Li D, Ma W, An R, Khan D, et al. Magnesium decreases aluminum accumulation and plays a role in protecting maize from aluminum-induced oxidative stress. Plant Soil. 2020;457(1):71–81.
43. Panda SK, Baluška F, Matsumoto H. Aluminum stress signaling in plants. Plant Signal Behav. 2009;4(7):592–7.
44. Wang P, Wan N, Horst WJ, Yang ZB. From stress to responses: aluminium-induced signalling in the root apex. J Exp Bot. 2023;74(5):1358–71.
45. Xu S, Wu L, Li L, Zhong M, Tang Y, Cao G, et al. Aluminum-induced alterations to the cell wall and antioxidant enzymes involved in the regulation of the aluminum tolerance of Chinese Fir (*Cunninghamia lanceolata*). Front Plant Sci. 2022;13:891117.
46. Ambachew D, Blair MW. Genome wide association mapping of root traits in the andean genepool of common bean (*Phaseolus vulgaris* L.) grown with and without aluminum toxicity. Front Plant Sci. 2021;12:628687.
47. Bityutskii NP, Yakkonen KL, Petrova AI, Shavarda AL. Interactions between aluminium, iron and silicon in *Cucumber sativus* L. grown under acidic conditions. J Plant Physiol. 2017;218:100–8.
48. de Sousa A, Saleh AM, Habeeb TH, Hassan YM, Zrieq R, Wadaan MAM, et al. Silicon dioxide nanoparticles ameliorate the phytotoxic hazards of aluminum in maize grown on acidic soil. Sci Total Environ. 2019;693:133636.
49. Xiao Z, Yan G, Ye M, Liang Y. Silicon relieves aluminum-induced inhibition of cell elongation in rice root apex by reducing the deposition of aluminum in the cell wall. Plant Soil. 2021;462(1):189–205.
50. Xiao Z, Liang Y. Silicon prevents aluminum from entering root tip by promoting formation of root border cells in rice. Plant Physiol Biochem. 2022;175:12–22.
51. Mabuchi K, Maki H, Itaya T, Suzuki T, Nomoto M, Sakaoka S, et al. MYB30 links ROS signaling, root cell elongation, and plant immune responses. PNAS. 2018;115(20):E4710–9.

52. Yamamoto Y, Kobayashi Y, Rama Devi S, Rikiishi S, Matsumoto H. Oxidative stress triggered by aluminum in plant roots. Plant Soil. 2003;255(1):239–43.
53. Salazar-Chavarría V, Sánchez-Nieto S, Cruz-Ortega R. Fagopyrum esculentum at early stages copes with aluminum toxicity by increasing ABA levels and antioxidant system. Plant Physiol Biochem. 2020;152:170–6.
54. Abo M, Yonehara H, Yoshimura E. Aluminum stress increases carbon-centered radicals in soybean roots. J Plant Physiol. 2010;167(15):1316–9.
55. Li W, Sun Y, Wang B, Xie H, Wang J, Nan Z. Transcriptome analysis of two soybean cultivars identifies an aluminum respon-sive antioxidant enzyme GmCAT1. Biosci Biotech Bioch. 2020;84(7):1394–400.
56. Sun C, Liu L, Zhou W, Lu L, Jin C, Lin X. Aluminum induces distinct changes in the metabolism of reactive oxygen and nitrogen species in the roots of two wheat genotypes with different aluminum resistance. J Agric Food Chem. 2017;65(43):9419–27.
57. Vega I, Nikolic M, Pontigo S, Godoy K, Mora MD, Cartes P, et al. Silicon improves the production of high antioxidant or structural phenolic compounds in barley cultivars under aluminum stress. Agronomy. 2019;9(7):388.
58. Sogarwal A, Kumari N, Sharma V. Role of silicon in abiotic stress tolerance in wheat. Cereal Res Commun. 2022;51:1–11.
59. Gill SS, Tuteja N. Reactive oxygen species and antioxidant machinery in abiotic stress tolerance in crop plants. Plant Physiol Biochem. 2010;48(12):909–30.
60. Zeng CQ, Liu WX, Hao JY, Fan DN, Chen LM, Xu HN, et al. Measuring the expression and activity of the CAT enzyme to determine Al resistance in soybean. Plant Physiol Biochem. 2019;144(2019):254–63.
61. Bilal S, Khan A, Imran M, Khan AL, Asaf S, Al-Rawahi A, et al. Silicon- and boron-induced physio-biochemical alteration and organic acid regulation mitigates aluminum phytotoxicity in date palm seedlings. Antioxid. 2022;11(6):1063.
62. Yu Y, Dong J, Li R, Zhao X, Zhu Z, Zhang F, et al. Sodium hydrosulfide alleviates aluminum toxicity in *Brassica napus* through maintaining H_2S, ROS homeostasis and enhancing aluminum exclusion. Sci Total Environ. 2023;858(2023):160073.
63. Zhang L, Liu R, Gung BW, Tindall S, Gonzalez JM, Halvorson JJ, et al. Polyphenol-aluminum complex formation: implications for aluminum tolerance in plants. J Agric Food Chem. 2016;64(15):3025–33.
64. Chen Y, Huang L, Liang X, Dai P, Zhang Y, Li B, et al. Enhancement of polyphenolic metabolism as an adaptive response of lettuce (*Lactuca sativa*) roots to aluminum stress. Environ Pollut. 2020;261(2020):114230.
65. Barceló J, Poschenrieder C. Fast root growth responses, root exudates, and internal detoxification as clues to the mechanisms of aluminium toxicity and resistance: a review. Environ Exp Bot. 2002;48(1):75–92.
66. Tolrà RP, Poschenrieder C, Luppi B, Barceló J. Aluminium-induced changes in the profiles of both organic acids and phenolic substances underlie Al tolerance in *Rumex acetosa* L. Environ Exp Bot. 2005;54(3):231–8.
67. Manquián-Cerda K, Cruces E, Escudey M, Zúñiga G, Calderón R. Interactive effects of aluminum and cadmium on phenolic compounds, antioxidant enzyme activity and oxidative stress in blueberry (*Vaccinium corymbosum* L.) plantlets cultivated *in vitro*. Ecotox Environ Safe. 2018;150:320–6.